Rev. Adv. Mater. Sci. 35 (2013) 39-47

MATERIAL VS DISCRETIZATION LENGTH SCALES IN PLASTICITY SIMULATIONS OF SOLID FOAMS

Xu Zhang[1,2,4], Katerina E. Aifantis[2,3,4] and Michael Zaiser[4]

[1]School of Mechanics and Engineering, Southwest Jiaotong University, China
[2]Laboratory of Mechanics and Materials, Aristotle University of Thessaloniki, Greece
[3]Civil Engineering-Engineering Mechanics, University of Arizona, Tucson, AZ, USA
[4]University of Erlangen, Department of Materials Science, Institute for Materials Simulation WW8, Dr.-Mack-Strasse 77, 90762 Fürth, Germany

Received: August 14, 2013

Abstract. The stress-strain response of metal foams has attracted significant attention from the mechanics community due to the local collapse that individual cells experience. This collapse results in the development of strain localization bands, also known as crushing bands, which give rise to a random but localized accumulation of damage. Such experimental observations have been successfully simulated by using a strain gradient plasticity model that is numerically implemented through a cellular automaton; stochasticity was accounted for by allowing the initial yield stress of each mesh element to vary according to a Weibull distribution. In the present study new simulations, along the same lines, are performed in order to further understand not only the effect of microstructure on the stress-strain response of ordered and disordered foams, but also that of the mesh size of the simulation grid. It is found that there are no significant size effects in foams of low disorder, while such effects exist when a higher degree of structural disorder is considered.

1. INTRODUCTION

Metal foams are used in a wide range of applications, mainly in the automotive and aerospace industries, due to their high energy absorption, high specific rigidity and high specific strength [1,2]. For such applications it is important to increase the durability and safety during use of the metal foam components, by tailoring their mechanical response, particularly during compression.

Experimental studies have revealed that there are usually three deformation stages during the compression of foams [3-6]. Initially, the whole sample deforms elastically, while after initial yielding the cellular structure collapses, giving a plateau in the stress-strain curve, which is followed by hardening. The collapse is initiated by fracture or elastic-plastic buckling of individual foam cells, which propagates through the material by narrow crushing bands. Such type of damage is localized and cannot be identified macroscopically by observing the stress-strain curves only [7-10]. This suggests that the intrinsic microstructural response to compression must be considered in order to capture both the micro and macroscopic mechanical behavior.

In doing so, previous studies [7,11] considered a gradient plasticity framework since it allows for the mechanical response of the individual foam to influence the neighboring cells and therefore, strain localization can propagate throughout the material in the form of bands. To account for the initiation of collapse in a single cell and subsequent band propagation, as well as for the disorder that is inherent to metal foams, the initial yield stress is taken to vary in each cell, according to a Weibull

Corresponding author: Katerina E. Aifantis, e-mail: aifantis@email.arizona.edu

distribution. To simulate such stochastic effects, the compressive strain gradient plasticity model is numerically implemented through a cellular automaton (CA). Such simulations have been able to successfully capture experimentally observed stress-strain curves, and to also predict the differences in the mechanical behavior between ordered versus disordered foams [11].

To further investigate the stress-strain response of cellular materials, and in particular size effects that result from their microstructure, simulations are performed herein for different types of foams in which either the cell size or overall specimen size was varied for both ordered and disordered foams. When one is concerned with simulations, however, the discretization length employed in the simulation, can also result in size effects, which are however simulation artifacts. Therefore we have separately studied the question of mesh size dependence and have investigated methods to remove mesh size related artifacts. These investigations provide some parameter analysis for the optimization and numerical realization of metal foams.

In the sequel the strain gradient plasticity formulation is first presented, followed by the investigation of size effects. In order to account for simulation artifacts, first it will be verified that the discretization length does not affect the stress-strain response, and then the effect of the cell size and specimen size will be considered.

2. STRAIN GRADIENT PLASTICITY MODEL FOR METAL FOAMS IN COMPRESSION

The mass conservation law and yield condition should be met by the deformed material under consideration. Hence, the evolution of the metal foam density is governed by the mass conservation law as

$$\dot{\rho} + \rho\,\mathrm{div}(\mathbf{v}) = 0 \Rightarrow \rho = \rho_0 e^{\left(-\mathrm{Tr}\,\boldsymbol{\varepsilon}\right)}, \tag{1}$$

where ρ_0 is the initial density of the metal foam and $\boldsymbol{\varepsilon}$ is the strain tensor whose first invariant $\mathrm{Tr}\,\boldsymbol{\varepsilon} = \varepsilon_{ij}$ represents the volume deformation. Part of the density is recoverable due to the elastic deformation, while the unrecoverable density $\tilde{\rho}$ resulting from the plastic compaction or buckling (characterized by the plastic strain tensor $\boldsymbol{\varepsilon}^{pl}$) can be written as

$$\tilde{\rho} = \rho_0 e^{\left(-\mathrm{Tr}\,\boldsymbol{\varepsilon}^{pl}\right)} \Rightarrow \rho = \tilde{\rho} e^{\left(-\mathrm{Tr}\,\boldsymbol{\varepsilon}^{el}\right)}. \tag{2}$$

Yielding and further plastic deformation of the metal foam occurs when the equivalent stress σ_{eq} is larger than the flow strength S,

$$\sigma_{eq} \geq S, \tag{3}$$

where we assume that the incremental strain is derived from an associated flow rule. According to the conventional plasticity for metals, deformation is not associated with volume changes, for metal foams however, volumetric changes play a crucial role in the initial deformation stages and therefore the equivalent stress is defined as [12,13],

$$\sigma_{eq} = \sqrt{\frac{3}{2}\sigma_{ij}^{dev}\sigma_{ij}^{dev} + \alpha\left(\sigma_{ii}\right)^2}. \tag{4}$$

The deviatoric stress tensor σ_{ij}^{dev} in Eq. (4) is denoted as $\sigma_{ij}^{dev} = \sigma_{ij} - 1/3\sigma_{ii}$, where summation is performed over the repeated indices. The non-dimensional parameter α determines the volumetric change that the foam experiences during deformation and it is chosen to be 0.5, for consistency with the experimental observation that there is no lateral expansion/contraction after uniaxial plastic deformation of many aluminum foams.

A phenomenological expression [14] for the yield function S in Eq. (3) is

$$S = S(\tilde{\rho}) = C\sigma_M \left(\frac{\tilde{\rho}}{\rho_M}\right)^2, \tag{5}$$

where $\tilde{\rho}$ is the stress-free density (i.e. the unrecoverable density in the unloaded status), and σ_M, ρ_M are the yield stress and density of the corresponding bulk metal material. The pre-factor C, which is related to the foam geometry and plastic buckling, is also further expressed in terms of $\tilde{\rho}$ as

$$C = C(\tilde{\rho}) = C_1 + \left(C_0 - C_1\right) e^{\left(-\frac{\tilde{\rho}-\rho_0}{\rho_1}\right)}, \tag{6}$$

where C_0 corresponds to the initial strength before compression, C_1 represents the reduced strength after compression, and ρ_1 is the characteristic density change associated with plastic buckling.

If we introduce the parameter $\eta = C_1/C_0$ for characterizing the relative reduction of the strength and the parameter $b^{-1} = \rho_1/\rho_0$ for representing the relative change of density, then combining Eqs. (5), (6), and (2) gives the final expression for the yield function as

$$S = S_0(\rho_0) g(\mathrm{Tr}\,\boldsymbol{\varepsilon}^{pl}), \tag{7}$$

where $S_0(\rho_0)$ is the initial yield stress that is a function of the initial density,

$$S_0 = S_0(\rho_0) = C_0\sigma_M \left(\frac{\rho_0}{\rho_M}\right)^2, \tag{8}$$

while $g(\mathrm{Tr}\,\boldsymbol{\varepsilon}^{\mathrm{pl}})$ represents the evolution of the yield stress and is a function of the plastic strain,

$$g(\mathrm{Tr}\,\boldsymbol{\varepsilon}^{\mathrm{pl}}) = \eta e^{-2\left(\mathrm{Tr}\,\boldsymbol{\varepsilon}^{\mathrm{pl}}\right)} + \left(1-\eta\right)e^{(b-2)\left(\mathrm{Tr}\,\boldsymbol{\varepsilon}^{\mathrm{pl}}\right)}. \tag{9}$$

Furthermore, to account for the strong interaction between adjacent cells of the metal foam, a spatial coupling term is introduced into the yield function through a gradient term [7,15] so that it becomes

$$S = S_0(\rho_0)g(\mathrm{Tr}\,\boldsymbol{\varepsilon}^{\mathrm{pl}}) - El^2\Delta\left|\mathrm{Tr}\,\boldsymbol{\varepsilon}^{\mathrm{pl}}\right|, \tag{10}$$

where Δ is the Laplace symbol which represents the second spatial gradient, E is the elastic modulus, and l is the internal length scale, which is inherent to gradient plasticity theories and is taken to be related to the cell size of the metal foam [7,11].

The microstructure parameters of metal foams (cell size, cell shape) are strongly fluctuating, resulting in spatial fluctuations of the density. Since the initial yield strength S_0 is a function of the density, it should also fluctuate in space. We describe this fluctuation using a Weibull distribution with shape parameter β and scale parameter Σ. The corresponding cumulative distribution function (CDF) is written as

$$F\left(S_0;\Sigma,\beta\right) = 1-\exp\left(-\left(\frac{S_0}{\Sigma}\right)^{\beta}\right) \tag{11}$$

and the probability density function (PDF) is given by

$$f(S_0;\Sigma,\beta)=\begin{cases}\dfrac{\beta}{\Sigma}\left(\dfrac{S_0}{\Sigma}\right)^{\beta-1}\exp\left(-\left(\dfrac{S_0}{\Sigma}\right)^{\beta}\right) & S_0 \geq 0,\\ 0 & S_0 < 0.\end{cases} \tag{12}$$

Thus, the initial yield strength can be further written as $S_0 = \bar{S}_0 + \delta S_0$, with the mean value of S_0 being $\bar{S}_0 = \Sigma\Gamma(1+1/\beta)$ and its variance $\overline{(\delta S_0)^2} = \Sigma^2\left[\Gamma\left(1+\frac{2}{\beta}\right)-\left(\Gamma\left(1+\frac{1}{\beta}\right)\right)^2\right]$. The coefficient of variation (COV) is

$$\mathrm{COV} = \frac{\sqrt{\overline{(\delta S_0)^2}}}{\bar{S}_0} = \sqrt{\frac{\Gamma\left(1+\frac{2}{\beta}\right)}{\left(\Gamma\left(1+\frac{1}{\beta}\right)\right)^2}-1}.$$

Uniaxial compression of metal foams is a one-dimensional problem. If we assume x as the loading axis, then $\sigma_{xx} := \sigma$ and $\varepsilon^{\mathrm{pl}}_{xx} = -e$ are the only non-zero components of the plastic strain tensor, thus

$$\sigma_{\mathrm{eq}} = \sqrt{\frac{3}{2}}\sigma,\ \mathrm{Tr}\,\boldsymbol{\varepsilon}^{\mathrm{pl}} = -e. \tag{13}$$

The yield condition expressed in Eq. (3) can therefore be written as

$$\sqrt{\frac{3}{2}}\sigma \geq S_0 g(-e) - El^2\Delta\left|-e\right|. \tag{14}$$

If we introduce the non-dimensional variables

$$\sqrt{\frac{3}{2}}\frac{\sigma}{\bar{S}_0} \rightarrow \sigma^*,\ \frac{S_0}{\bar{S}_0} \rightarrow S_0^*,\ \frac{E}{\bar{S}_0} \rightarrow E^*$$

and $x/l \rightarrow x^*$, then

$$\sigma^* \geq S_0^*\left(\eta e^{2e} + \left(1-\eta\right)e^{((2-b)e)}\right) - E^* e_{,x^*x^*}. \tag{15}$$

S_0^* then obeys a new Weibull distribution with non-dimensional parameters $\Sigma^* = \Sigma/\bar{S}_0$ and β. Now the cumulative distribution function (CDF) is

$$F(S_0^*;\Sigma^*,\beta) = 1-\exp\left(-\left(\frac{S_0^*}{\Sigma^*}\right)^{\beta}\right) \tag{16}$$

and the probability density function (PDF) is

$$f(S_0^*;\Sigma^*,\beta)=\begin{cases}\dfrac{\beta}{\Sigma^*}\left(\dfrac{S_0^*}{\Sigma^*}\right)^{\beta-1}\exp\left(-\left(\dfrac{S_0^*}{\Sigma^*}\right)^{\beta}\right) & S_0^* \geq 0,\\ 0 & S_0^* < 0,\end{cases} \tag{17}$$

The corresponding average value equals 1 and the COV remains

$$\sqrt{\frac{\Gamma\left(1+\frac{2}{\beta}\right)}{\left(\Gamma\left(1+\frac{1}{\beta}\right)\right)^2}-1}.$$

Eq. (15) is solved using a cellular automaton method. The whole sample with dimensionless size of $L/l \rightarrow L^*$ is divided into N sections/ mesh elements (similar to the elements in the finite element method) with the mesh size being $\xi = L/N$ and its corresponding non-dimensional version being $\xi^* = L^*/N$. The corresponding geometrical configuration is shown in Fig. 1.

The yield status is determined by evaluating Eq. (15) in each discrete mesh element labeled by

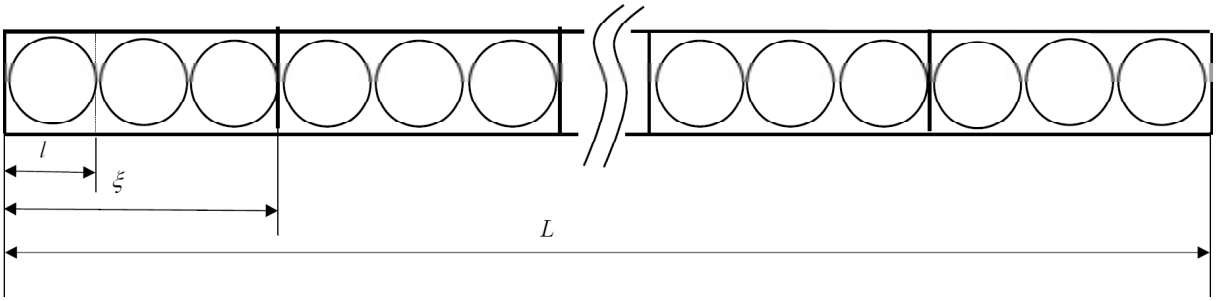

Fig. 1. The geometrical configuration for a metal foam simulated using a cellular automaton model with the average cell size l, mesh length ξ and sample size L. Here the model with non-dimensional $\xi^*=3$ is schematically illustrated.

index *i.* The gradient term in cell *i* is numerically approximated by the finite difference

$$\left[e_{,x^*x^*}\right]_i = \frac{\left[e_{,x^*}\right]_i - \left[e_{,x^*}\right]_{i-1}}{\xi^*} = \frac{1}{\xi^*}\left(\left[\frac{e_{i+1}-e_i}{\xi^*}\right] - \left[\frac{e_i - e_{i-1}}{\xi^*}\right]\right) = \frac{1}{\left(\xi^*\right)^2}\left(e_{i+1}+e_{i-1}-2e_i\right). \tag{18}$$

The initial yield strength for element *i* follows the Weibull distribution, and the corresponding value is evaluated numerically as

$$\left[S_0^*\right]_i = \Sigma^*\left[-\ln R_i\right]^{1/\beta}, \tag{19}$$

where R_i is an equidistributed random number ranging from 0 to 1.

According to the balance equation $\sigma_{ij,i} = 0$, the axial stress in the compressed metal foam is a constant, which is equal to the overall stress, and is determined by

$$\sigma_i^* = E^*\left(e_{tot} - \frac{1}{N}\sum_{i=1}^{N} e_i\right). \tag{20}$$

Substituting Eqs. (20), (19), and (18) into Eq. (15), provides the final numerical formulation, which we use to evaluate the deformation behavior of the compressed metal foam, as

$$E^*\left(e_{tot} - \frac{1}{N}\sum_{i=1}^{N} e_i\right) > \Sigma^*\left[-\ln R_i\right]^{1/\beta}\left(\eta e^{2e_i} + (1-\eta)e^{(2-b)e_i}\right) - \frac{E^*}{\left(\xi^*\right)^2}\left(e_{i+1}+e_{i-1}-2e_i\right). \tag{21}$$

This equation is the core equation, which will be implemented numerically to analyze the mechanical properties of compressed metal foams. The values for the parameters that are required to run the simulations are obtained from Blazy's experimental investigation of aluminum foams [16]. Particularly, the initial elastic modulus and yield strength are 110 MPa and 5.5 MPa, respectively, thus the non-dimensional elastic modulus is $E^* = 20$. The compressive behavior of metal foams is always affected by the plastic buckling. It's assumed that the plastic buckling occurs when the density change exceeds 5% of the initial density, thus $b = 20$, and the corresponding relative strength reduction is $\eta = 0.47$

During the simulation, the total strain is increased in small steps from 0 to 1. The step size is taken to be 0.004 so as to have a fine resolution for the plotted stress-strain response. In each step, the yield condition is evaluated for the discrete mesh elements, and the local plastic strain e_i is increased by a small amount of 0.0004 for any element *i*, fulfilling the yield condition. Then, the global stress is adjusted according to Eq. (20) and the yield condition (Eq. (21)) is re-evaluated for all mesh elements. This procedure is repeated iteratively until no yield occurs anywhere. In order to obtain the average stress-strain curve, 500 simulations are performed and averages are taken.

3. SIZE EFFECT FOR COMPRESSED METAL FOAMS WITH LOW DISORDER

For the metal foam with low disorder, β is taken to be 10. Then the corresponding COV is calculated to be 0.12. In order to meet the requirement that the mean value of $\overline{S_0^*}$ is 1, Σ^* is calculated to be 1.05.

Using the aforementioned materials parameters, the effects that the sample size, cell size, and

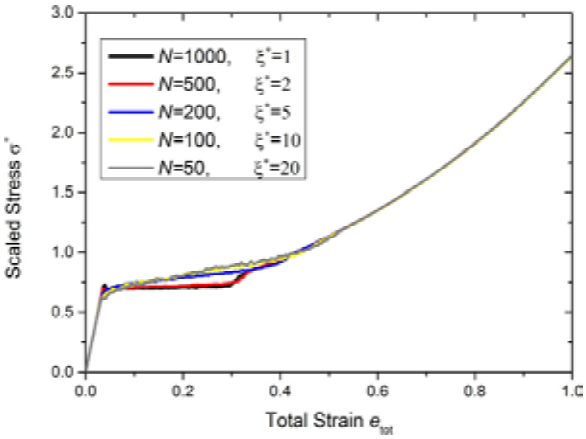

Fig. 2. The mesh size effect for metal foams with low-disorder microstructure.

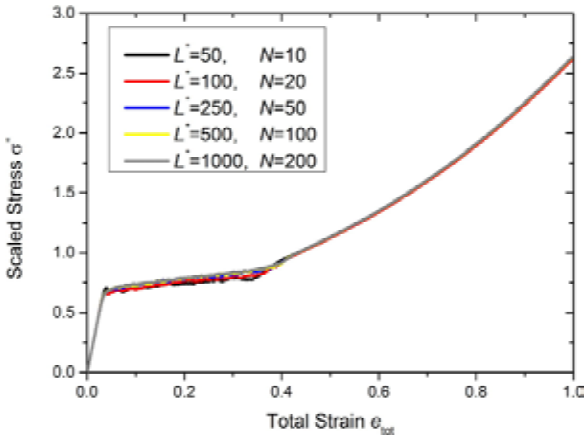

Fig. 3. The sample size effect for metal foams with low-disorder microstructure.

discretization length (i.e. mesh element size) have on the mechanical response of metal foams are investigated as follows:

(1) Varying the mesh size

In the first case examined, the sample size (L) and the average cell size (l) were kept constant, L = 2600 mm and l = 2.6 mm, while the number of mesh elements N was allowed to vary, corresponding to a change of the mesh size ξ. The parameters used in the simulations are summarized in Tables 1(a)&(b). The corresponding simulation results for an aluminum metal foam with low disorder are summarized in Fig. 2. It is seen that the mesh size does not affect the stress-strain response of low disorder foams.

(2) Varying the sample size

In the second set of simulations performed, the average cell size (l) and the discretization length (ξ) were kept constant; l = 2.6 mm and ξ = 13 mm, respectively. The specimen size (L) was allowed to range from 130 mm to 2600 mm, in order to investigate the effect of sample size. Hence, the number of mesh elements N increased with the specimen length. The dimensional and, respective, non-dimensional parameters characterizing the foams under consideration are shown in Table 2(a)&(b). Fig. 3 illustrates the response of a low disorder aluminum foam.

(3) Varying the cell size

In the third set of simulations the specimen size and discretization length were kept constant, L = 520 mm, and ξ = 5.2, while the cell size ranged from 0.52 mm to 5.2 mm. The parameters for the investigated sample are summarized in Tables 3(a)&(b). Fig. 4 illustrates the simulation results for an aluminum metal foam whose microstructure exhibits low disorder for different specimen sizes.

Figs. 3 and 4 indicate that no size effects exist when the foam microstructure is characterized by low disorder, regardless of whether the cell size or sample size was varied.

In the metal foam with low disorder, the cell size and the resulting yield strength were distributed in a narrow band. The initial yield strength with Weibull

Table 1. The parameters used in the investigation of discretization length effect. (a) with unit, (b) non-dimensional parameters.

(a)

L (mm)	2600	2600	2600	2600	2600
l (mm)	2.6	2.6	2.6	2.6	2.6
ξ (mm)	2.6	5.2	13	26	52

(b)

L^*	1000	1000	1000	1000	1000
N	1000	500	200	100	50
ξ^*	1	2	5	10	20

Table 2. The parameters used in the investigation of specimen size effect. (a) with unit, (b) non-dimensional parameters.

(a)

L (mm)	130	260	650	1300	2600
l (mm)	2.6	2.6	2.6	2.6	2.6
ξ (mm)	13	13	13	13	13

(b)

L^*	50	100	250	500	1000
N	10	20	50	100	200
ξ^*	5	5	5	5	5

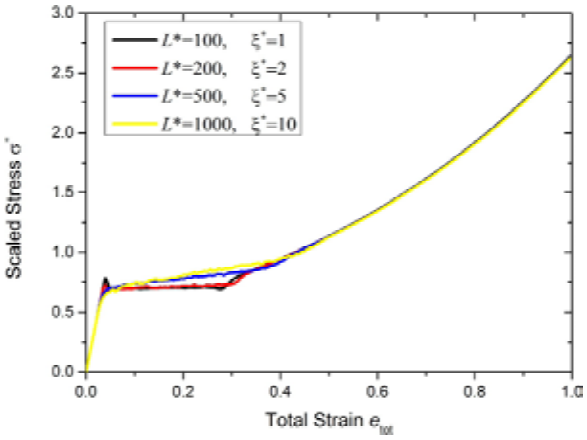

Fig. 4. The cell size effect for metal foams with low-disorder microstructure.

parameter $\beta = 10$ exhibited a comparatively narrow distribution where the standard deviation of $[S_0^*]_i$ in Eq. (19) was only 0.12 of the mean value 1. Thus, the gradient term contribution dominated the deformation behavior, resulting in a propagation-controlled deformation mode characterized by a stress plateau after yielding. Specifically, the collapse bands nucleate at the weakest mesh elements and then propagate to the neighboring ones. The propagation of the bands is assisted by the strain gradient in the band front so as to overcome the higher yield stress of the neighboring elements, and the plateau stress, as well as the length of the plateau, are determined by the Maxwell construction (equal area rule) for the constitutive model of the softening-hardening type as discussed in [11,17] for analogous problems. After the plateau, deformation is indeed homogenous, and compaction continues at a rapidly increasing stress, which follows the hardening regime of the softening-hardening model introduced in Eq. (9). The whole macroscopic stress-strain response of the low disordered metal foam is similar to the softening-hardening model, since the gradient term dominates over the disorder in such cases. The only effect of the disorder is to facilitate band nucleation and, thus, to eliminate the initial yield point often associated with constitutive laws of the softening-hardening type.

4. SIZE EFFECT FOR COMPRESSED METAL FOAMS WITH HIGH DISORDER

For the metal foam with high disorder, β is taken to be 0.25; thus the corresponding COV is calculated to be 8.31. This corresponds to foams with a highly disordered, fractal, structure, as the distribution of

Table 3. The parameters used the investigation of cell size effect. (a) with unit, (b) non-dimensional parameters.

(a)

L (mm)	520	520	520	520
l (mm)	5.2	2.6	1.04	0.52
ξ (mm)	5.2	5.2	5.2	5.2

(b)

L^*	100	200	500	1000
N	100	100	100	100
ξ^*	1	2	5	10

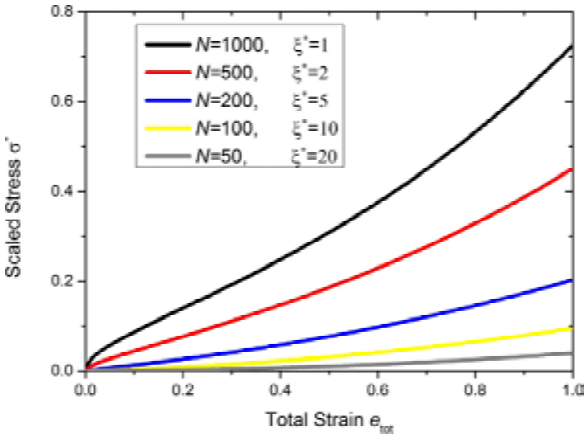

Fig. 5. The mesh size effect for metal foams with highly disordered microstructure ($\beta = 0.25$).

the "cell sizes" is a truncated power law. (For other fractal microstructures with similar strength distribution, see [18].) In order to meet the requirement that the mean value $\overline{S_0^*}$ is 1, Σ^* is calculated to be 0.04. All other parameters are assumed to have the same values as for the low disordered metal foam.

(1) Varying the mesh size

In investigating the effect of the discretization length in highly disordered metal foams, we consider the case of large samples where the results are independent on sample size (cf. (2) below). We can therefore attribute the significant changes in the deformation behavior seen in Fig. 5 exclusively to the change in size of the mesh elements. At first glance the observation of such mesh dependence is very worrying – since the mesh size is a purely numerical parameter of the model and its change should not affect the material behavior.

To understand the origin of this problem, we need to look at the physical meaning of the non-dimensional mesh size: ξ^* represents how many

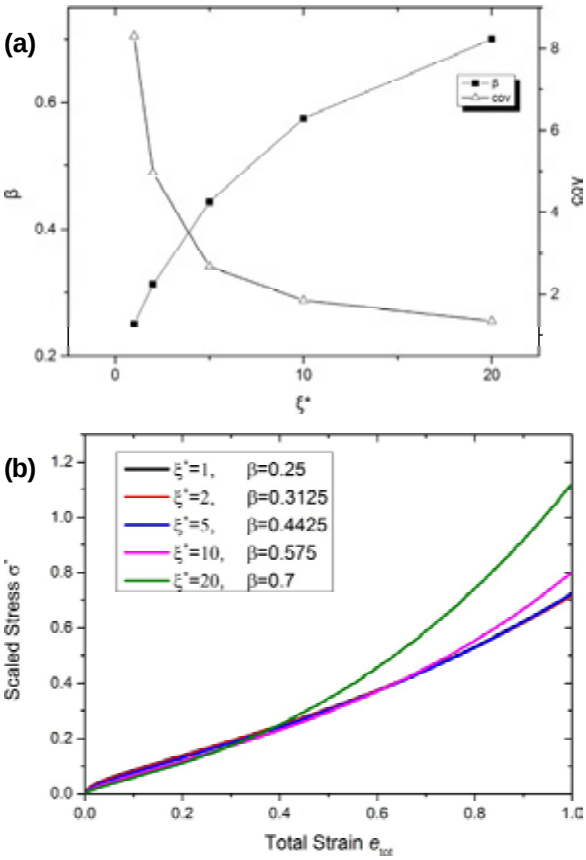

Fig. 6. (a) Modification of the Weibull distribution parameter b and COV to compensate the effect of changing mesh length ξ*. (b) The mesh size effect of highly disordered metal foams with modified β.

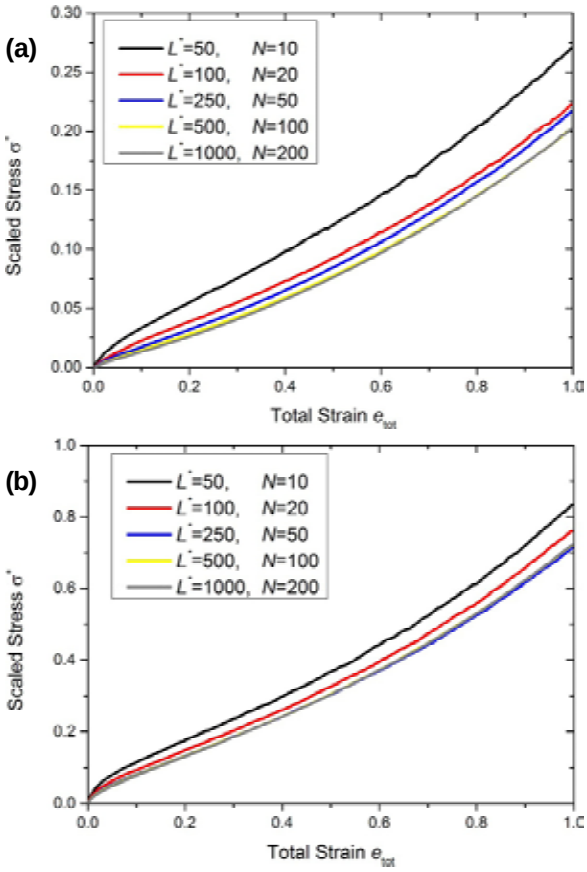

Fig. 7. The specimen size effect of metal foams with highly disordered microstructure. (a) β = 0.25, (b) β = 0.4425.

cells are included in one mesh element. By construction, all the cells in the mesh element share the same initial yield stress in the cellular automaton simulation. If we lump many cells of the physical microstructure into one element, then the yield stress of the assembly should have less scatter than if one element contains only a small number of cells. Conversely, if we use elements of different size, but characterize them with the same disorder parameter, then the simulations with larger elements actually represent different (more disordered) microstructures than those with smaller element size. Accordingly, the results of Fig. 5 indicate that the latter are weaker than the former. Only in the limit $\xi^* = 1$, the scatter of the mesh element strength distribution directly reflects the real microstructure disorder and the resulting fluctuations of initial yield stresses.

To mitigate this problem and achieve a representation of the deformation behavior that is independent on the choice of discretization length, the parameters of the Weibull distribution need to be rescaled, together with the change of the non-dimensional mesh element size ξ^*, such as to represent the same deformation behavior. In this manner we may eliminate the mesh size dependence of the macroscopic stress-strain response, which is also the requirement of a stable simulation method.

The required change of the Weibull distribution parameter β with the change of ξ^* is shown in Fig. 6a. The new simulation results shown in Fig. 6b indicate that the mesh size dependence can be eliminated by modifying the disorder parameter β with the change of ξ^* when ξ^* is smaller than 10, while the mesh size dependence will always persist for larger ξ^*.

Thus, there exists an intrinsic upper limit to the scalability of the model. This is indeed true for all gradient models with or without stochasticity. If applied to strain softening materials, there is an upper length scale above which the results must become mesh dependent. For gradient plasticity of a material with softening, we get localized deformation bands, which have an intrinsic width that relates to the internal length scale. For softening-hardening we get a propagating band (see

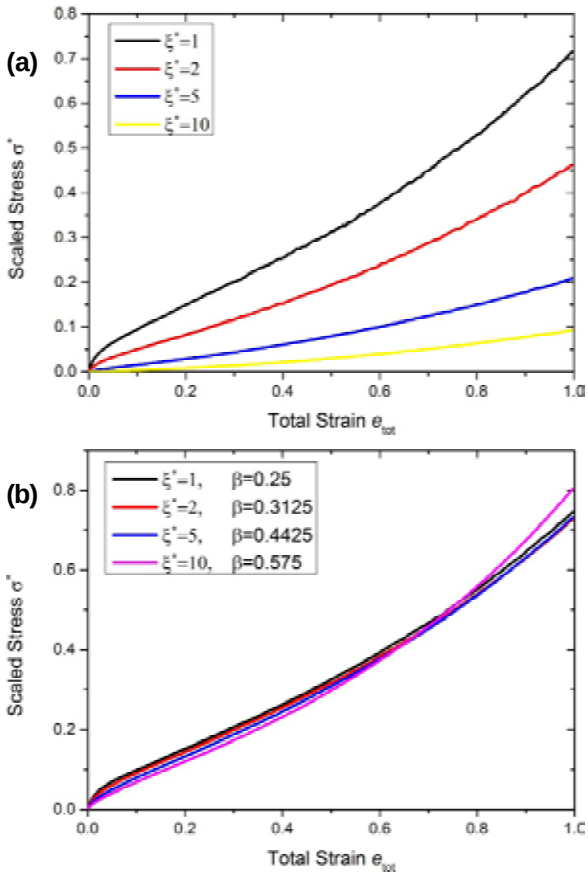

Fig. 8. The cell size effect of metal foams with highly disordered microstructure. (a) β=0.25, (b) after modification of β to compensate the mesh size effect.

plastic strain profile in [11]) with a band front width w that is again intrinsic to the material parameters. In the simulation for $\xi^* = 1$, the non-dimensional band width (or band front width) is about $w^* = w/l = 10$, in other words, it is about 10 cell sizes. Mesh independence means that the band width w^* does not depend on the mesh size ξ^*. Quite evidently, a band of width $w^* = 10$ cannot be represented if the mesh size is equal to or larger than this value. As the intrinsic spatial structure of the deformation patterns can no longer be represented with coarser meshing, a scale dependence of the simulation results is to be expected since the spatial interactions between adjacent volume elements can no longer be adequately represented.

To summarize: increasing ξ^* reduces the coupling between mesh elements (gradient term effect, see Eq. (21)) and therefore makes the material appear more disordered -since the gradient term (which wants to homogenize deformation by propagating a band) now carries less and less weight while the disorder remains the same. One can balance this by reducing the disorder (increasing β), however this works only as long as one can correctly represent the action of the gradient term at all, i.e. for $\xi^* < 10$. Above $\xi^* = 10$ the model can no longer correctly represent the strain pattern even without disorder, so discretization artifacts are bound to occur.

(2) Varying the sample size

Now the effect of the specimen size on the stress-strain response was examined. The parameters listed in Table 2 were used and the simulation results are shown in Fig. 7a. The results indicate that a size effect exists when L is smaller than 500. For larger systems (L>500), there is no size effect. It thus seems that there is a critical value of L, above which the size effect disappears. This is consistent with the classical idea that the behavior of a heterogeneous material should become scale invariant above the scale of some "representative volume". In order to investigate the dependence of the critical value of L on the disorder parameter β, another case with decreased disorder (β = 0.4425, keeping the mean value at 1) was investigated, and the corresponding results are shown in Fig. 7b. It is seen that in this case a sample size effect exist only when L is smaller than 250, above which there is no size effect. Thus, the critical value of L decreases with decreasing disorder – which is intuitively obvious. Recall also that there is no size effect in low disordered metal foams with β = 10.

In the size effect regime (e.g. $L^* = 50, 100, 250, 500$ for the β = 0. 25 case), it's further noted that a trend is observed, according to which "larger" samples have a "weaker" stress-strain response (the stress-strain curves are located at lower stresses for the same strain). The low value of β in the Weibull distribution of the initial yield stress results in a highly heterogeneous distribution of $[S_0^*]_i$, which also varies over a wide range of values. Thus, the increase on the number of cells will increase the probability that cells have very low initial yield stresses. Thus, the flow stress in highly disordered metal foams decreases as L increases.

(3) Varying the cell size

For the investigation of the effect that the cell size has, the number of mesh elements is kept constant at $N = 100$, while the dimensionless mesh size ξ^* is allowed to vary. This implies that we consider geometrically similar specimens: the cell size and the specimen size are proportional to each other. Fig. 8a shows that despite the geometrical similarity, changing ξ^* results in significant changes in the deformation behavior. However, these changes are offset once we re-normalize the disorder to account for the changing non-dimensional mesh size

according to Fig. 6a. Using the modified β, no significant cell size dependence is observed, as shown in Fig. 8b, which is expected since proportional scaling of all microstructural parameters should produce materials with identical deformation behavior.

5. CONCLUSION

The effects of varying the cell size, specimen size, and mesh size in metal foams that are characterized by low and high microstructural disorder, were investigated using a strain gradient plasticity framework that was solved numerically using a cellular automaton. Stochastic effects were accounted for by allowing the initial yield stress of the mesh elements to vary according to a Weibull distribution. For foams that are characterized by a low disorder it was seen that the stress-strain curves were not affected either by the specimen size or by the mesh length. However, significant size effects were obtained for highly disordered foams, when the specimen size was varied, following the "the smaller the stronger" paradigm. Furthermore, an unexpected mesh dependence in the stress-strain response was observed in highly disordered foams, which, however, could be eliminated through the modification of the yield stress fluctuations with the change of the mesh size. Similarly, the observed cell size dependence of the mechanical behavior of disordered foams, can be eliminated by appropriate re-scaling of the yield stress fluctuations, reflecting the fact that specimens of different cell size but similar density are geometrically similar and should therefore show identical deformation behavior. This points at an issue of general importance for deformation models which include stochastic fluctuations into discretized plasticity models. In order to prevent such models from displaying spurious mesh size dependence of the simulation results, the stochastic model must be complemented by a scaling rule which tells how the statistics depends on the ratio between the discretization length and the physical length scale of the underlying material microstructure.

ACKNOWLEDGEMENT

The authors are grateful to KEA's European Research Council Starting Grant MINATRAN 211166 for its support. Xu Zhang is grateful to the supports by NSFC (11202172), CPSF (2013M530405), and the Fundamental Research Funds for the Central Universities (SWJTU11CX072).

REFERENCES

[1] J. Baumeister, J. Banhart and M. Weber // *Materials & design* **18** (1997) 217.
[2] L.J. Gibson and M.F. Ashby, *Cellular solids: structure and properties* (Cambridge university press, 1999).
[3] H. Bart-Smith, A.F. Bastawros, D.R. Mumm, A.G. Evans, D.J. Sypeck and H.N.G. Wadley // *Acta Mater* **46** (1998) 3583.
[4] A.F. Bastawros, H. Bart-Smith and A.G. Evans// *J Mech Phys Solids* **48** (2000) 301.
[5] D. Weaire and M.A. Fortes// *Advances In Physics* **43** (1994) 685.
[6] A.-H. Benouali, L. Froyen, T. Dillard, S. Forest and F. N'guyen// *Journal of materials science* **40** (2005) 5801.
[7] K.E. Aifantis, A. Konstantinidis and S. Forest // *Journal of Computational and Theoretical Nanoscience* **7** (2010) 360.
[8] S. Forest, J.-S. Blazy, Y. Chastel and F. Moussy // *Journal of materials science* **40** (2005) 5903.
[9] M. Doyoyo and T. Wierzbicki // *Int J Plast* **19** (2003) 1195.
[10] T. Wierzbicki and M. Doyoyo // *Journal of applied mechanics* **70** (2003) 204.
[11] M. Zaiser, F. Mill, A. Konstantinidis and K.E. Aifantis // *Materials Science and Engineering: A* **567** (2013) 38.
[12] V.S. Deshpande and N.A. Fleck // *J Mech Phys Solids* **48** (2000) 1253.
[13] X.H. Zhu, J.E. Carsley, W.W. Milligan and E.C. Aifantis // *Scr Mater* **36** (1997) 721.
[14] C. Park and S.R. Nutt // *Mater Sci Eng A* **299** (2001) 68.
[15] E.C. Aifantis // *International Journal of Engineering Science* **22** (1984) 961.
[16] J.-S. Blazy, A. Marie-Louise, S. Forest, Y. Chastel, A. Pineau, A. Awade, C. Grolleron and F. Moussy // I*nternational journal of mechanical sciences* **46** (2004) 217.
[17] E.C. Aifantis and J.B. Serrin // *Journal of Colloid and Interface Science* **96** (1983) 530.
[18] P. Hähner and M. Zaiser // *Mater Sci Eng A* **272** (1999) 443.